This is the Pre-Published Version.
Engineering Applications of Artificial Intelligence 25 (8): 1670-1676 2012

Artificial Neural Network simulation of hourly groundwater levels in a coastal aquifer system of the Venice lagoon.

Riccardo Taormina[1], *Kwok-wing Chau*[1*], *Rajandrea Sethi*[2]

[1] Department of Civil and Structural Engineering, Hong Kong Polytechnic University, Hung Hom, Kowloon, Hong Kong, People's Republic of China

[2] DIATI - Dipartimento di Ingegneria dell'Ambiente, del Territorio e delle Infrastrutture, Politecnico di Torino, Corso Duca degli Abruzzi 24, 10129, Turin, Italy

*Corresponding author (email: cekwchau@polyu.edu.hk)

Abstract

Artificial Neural Networks (ANNs) have been successfully employed for predicting and forecasting groundwater levels up to some time steps ahead. In this paper, we present an application of feed forward neural networks (FFNs) for long period simulations of hourly groundwater levels in a coastal unconfined aquifer sited in the Lagoon of Venice, Italy. After initializing the model with groundwater elevations observed at a given time, the developed FNN should able to reproduce water level variations using only the external input variables, which have been identified as rainfall and evapotranspiration. To achieve this purpose, the models are first calibrated on a training dataset to perform 1-hour ahead predictions of future groundwater levels using past observed groundwater levels and external inputs. Simulations are then produced on another data set by iteratively feeding back the predicted groundwater levels, along with real external data. The results show that the developed FNN can accurately reproduce groundwater depths of the shallow aquifer for several months. The study suggests that such network can be used as a viable alternative to physical-based models to simulate the responses of the aquifer under plausible future scenarios or to reconstruct long periods of missing observations provided past data for the influencing variables is available.

Keywords:

Artificial neural networks, groundwater levels, coastal aquifer system, Venice lagoon, simulation.

1. Introduction

The simulation of hydraulic heads fluctuations in groundwater systems is generally carried out by means of *physical-based models*, which demand a proper synthesis of the aquifer parameters to describe the spatial variability of the subsurface. This information is hard to obtain even with expensive site investigations, and the partitioning of the physical domain required for the numerical solution may result in extreme computational costs. Although developing a rigorous numerical model of the flow system is preferable, as it entails a deeper understanding of the aquifer dynamics, when the focus is on the model outputs these issues may be overcome by employing *black box* empirical models. Black boxes perform a mathematical mapping between historical inputs and outputs without requiring physical information on the investigated system. Among these heuristics, artificial neural networks (ANNs) have been widely used in the field of hydrology (ASCE Task Committee on Application of Artificial Neural Networks in Hydrology, 2000). In particular, feed-forward neural networks (FNNs) have been applied successfully for time series modelling in many hydrological contexts such as rainfall-runoff (Dawson and Wilby, 1998; Hsu et al., 1995), river flow (Cheng et al., 2005; Joorabachi et al., 2007), flood forecasting (Chau et al., 2005), and water quality modelling (Muttil and Chau, 2006; May and Sivakumar, 2009). A detailed review of ANNs applications for modelling water resource variables can be found in Maier and Dandy (2000) and Maier et al. (2010). Relevant applications for prediction and forecasting water table depth time series are also available in the literature. Coulibaly et al. (2001) used different types of ANNs for monthly predictions of groundwater levels in the Gondo Plain, Burkina Faso. The study has shown that ANNs are an effective tool for up to 3 months ahead forecasting of the dry season deep water table depths, and can be employed for water management in semiarid areas. Daliakopoulos et al. (2005) tested the performance of several types of ANNs and training algorithms to forecast monthly groundwater fluctuations in an aquifer in the Messara Valley, Crete, up to 18 months ahead. The best results were obtained with the feed forward neural network architecture trained with the

Levenberg-Marquardt algorithm. Nayak et al. (2006) employed ANN for forecasting monthly levels in two different wells of an unconfined coastal aquifer in Godavari Delta System, India. Their study suggests that accurate monthly forecasting up to 4 months ahead can be obtained with relatively simple networks, provided the an accurate identification of the system inputs is carried out beforehand. Trichakis et al. (2009) employed artificial neural networks for daily forecasting of the water stage of a karstic aquifer in the region of Attica, Greece. Their findings suggests that major improvements in the neural network predictive performance could be achieved by employing the groundwater head variation between two time steps instead of the hydraulic head as the output variable. When observations from a network of piezometers are available, neural networks can also be employed for modeling the spatial variations in the water table. Nourani et al. (2008, 2011) employed artificial neural networks for spatio-temporal prediction of groundwater levels in the Tabriz and Shabestar plain, northwest Iran. Their results show that neural networks can be employed either as a replacement or in conjunction with existing geostatistical models to increase the performances of spatio-temporal water table predictions for complex multilayered aquifers.

In most of the available literature, artificial neural networks have been employed to reproduce groundwater levels on a monthly or daily basis, since such time resolutions are usually appropriate for most hydrogeologic situations and water management applications. However, in this work we deal with a shallow and very responsive aquifer, for which major changes in the water table levels suddenly occur due precipitation after storm events. The object of this study is thus to check whether neural models are capable of accurately reproduce the variation of groundwater levels on a hourly basis, with particular focus on their performances over long period simulations. The case study is a coastal aquifer sited in the Venetian Lagoon (Italy), where a defence system (Mo.S.E. system) is being developed to protect the inland from high tides (Bras et al., 2001; Rinaldo et al., 2008). A network of piezometers has been subsequently emplaced in the study area to monitor the effects of construction works on groundwater dynamics (Magistrato delle Acque di Venezia, 2008). As mentioned before, the depth to groundwater found in the aquifer is usually low, and the aquifer is highly responsive to rainfall infiltration. High-frequency monitoring of the water table is then required for detecting the sudden rises occurring after storms, i.e. for issuing flooding warnings if the levels are beyond the safety thresholds. A neural network is then employed to model such high-frequency variations on a hourly basis and produce long term simulations of groundwater levels. Simulations are obtained by using only observed data for the influencing external variables, rainfall and evapotranspiration, as direct inputs as well as past predicted values of the groundwater head as recursive inputs. Therefore the model can be harnessed for reconstructing the aquifer responses under plausible future scenarios or to reconstruct long periods of missing observations provided past data for the influencing variables is available.

2. Feed-forward neural networks (FNN)

Feed forward neural networks are biologically inspired distributed parallel processors which are known to approximate any continuous function with an arbitrary degree of accuracy (Hornik et al., 1989).These heuristics are particularly suited for predicting and forecasting hydrologic variables because of their ability to model nonlinear, nonstationary and nongaussian processes like those encountered in hydrological contexts (Maier and Dandy, 1997). FNNs consist of a number processing *units*, or *neurons*, linked by *synaptic connections* and arranged in *layers*. The inputs are fed through the input layer and, after being multiplied by synaptic weights, are delivered to the first hidden layer. In the hidden units, the weighted sum of inputs is transformed by a nonlinear activation function, which is usually chosen as the logistic or the hyperbolic tangent. The same process takes place in each of the following hidden layers, until the outcomes reach the output nodes. In this work, all the developed FNN models will have one hidden layer and will be fully connected, i.e. each node of the previous layer is linked to each node of the next layer. For further details on FNNs the reader is referred to the bibliography (Haykin, 1998; ASCE Task Committee on Application of Artificial Neural Networks in Hydrology, 2000). However, for the remaining of the discussion here, it is worth noting that the scalar predicted output $\hat{y}_t$ of a FNN with one output node is a function

$$\hat{y}_t = f(\mathbf{x}_t, \mathbf{w}), \quad (1)$$

where **w** is the ensemble of the synaptic weights and $\mathbf{x}_t$ the input variables currently fed to the network. After initializing the synaptic weights, the model calibration, or *training* in ANNs jargon, is performed by minimizing an error function of the predicted and the observed outputs on a given data set. If $\mathbf{Z} = [\mathbf{x}_t, y_t]$, t = 1 … N is the training data set made of N input-output pairs, and the error function is chosen as the sum of the nonlinear least squares

$$E(\mathbf{w}) = \frac{1}{2}\sum_{t=1}^{N}\left(y_t - \hat{y}_t(\mathbf{x}_t, \mathbf{w})\right)^2, \quad (2)$$

then the optimization is achieved by searching the optimal set of weights $\tilde{\mathbf{w}}$ such that

$$\tilde{\mathbf{w}} = \arg\min E(\mathbf{w}) = \arg\min\left(\frac{1}{2}\sum_{t=1}^{N}\left(y_t - \hat{y}_t(\mathbf{x}_t, \mathbf{w})\right)^2\right) \quad (3)$$

This search is usually performed using first-order or second-order optimization algorithms, with the latter being preferred because of being faster and more reliable. In particular, in this study the developed FNNs will be trained using the second-order Levenberg-Marquardt method (Coulibaly et al., 2000).

3. Case Study

The case study area is located in Punta Sabbioni, the edge of the Cavallino coastal strip of the Venetian Lagoon (Figure 1a). The strip is part of the system of coastlines that constitutes the natural barrier protecting the City of Venice from the open sea. The study area is facing the Lido inlet, which is the widest of the three openings connecting the lagoon with the Adriatic sea. In Punta Sabbioni, two different aquifer layers of silty sands can be identified, separated by an aquiclude of clayed silt around 5 meters thick, which is deemed to prevent vertical flow between the aquifers. The depth to groundwater of the shallow aquifer is very low, being usually between 0.6 and 1.8 meters. The water table is thus very susceptible to the effects of the natural driving forces, which also regulate groundwater flow throughout the year. Evapotranspiration in summer causes strong decrease in the water levels which, in turn, engenders a net water flow from the sea to the inland. This effect is reversed in the autumn when heavy rainfalls recharge the aquifer. Apart from the natural forces, other influences on groundwater dynamics may result from past and current anthropic activities in the area. In the past, for land reclamation purposes, a dense network of secondary channels and gullies was built to drain the excess water in Punta Sabbioni. Due to their limited size, however, flow in these channels is assumed not to influence the levels in the shallow aquifer. Other disturbances might be engendered by works undergoing in the nearby construction site in Figure 1b. These activities are included in the design of the high-water defence system (Mo.S.E. system) which, after its completion, is meant to protect the population and cultural heritage of the City of Venice from high waters (Bras et al., 2001; Magistrato delle Acque di Venezia, 2008; Rinaldo et al., 2008). The defence system includes mobile flood gates realized at the lagoon inlets and a series of complementary works capable of abating the level of the most frequent tides. In Punta Sabbioni works are taking place to build a navigation lock for small vessels. The project entails complete isolation of the construction site by emplacement of diaphragms along the perimeter and subsequent dewatering by means of a set of pumping wells. The site has to be kept dry also because it will be used for the precasting of the reinforced concrete panels constituting the flood gates in Lido inlet.

4. Observed data

4.1. Groundwater table depth

In order to monitor the effects of the dewatering process on groundwater dynamics, a network of 11 piezometers intercepting both aquifers has been drilled in the study site (Figure 1b). The monitoring network covers an area of about 1 km^2, and the distance between each piezometer and the coast varies from 10 to 500 meters. The groundwater head is recorded every 10 minutes by water level transducers. These observations are then processed to eliminate the effects of the atmospheric pressure measured by barometric sensors, and then averaged to produce hourly time series. The height of the water table is always referred to the average sea level as provided by the national marigraphic network of Italy. From a cursory analysis of the recordings, pumping operations are found to affect only the deeper aquifer, as the separating aquiclude prevents drawdowns in the shallow one. Therefore, pumping discharges are not needed for modelling hydraulic head fluctuations in the unconfined aquifer of interest. Two different behaviours of the water table are identified depending on the distance from the sea. In fact, the groundwater head in the piezometers placed by the coastline is heavily influenced by the marine tide, whereas groundwater dynamics for the inward piezometers depends on rainfall recharge and evapotranspiration. For the remainder of the discussion, we will be concerned only with the time series of the inward piezometers, being those relative to the piezometers near the coast entirely driven by tidal oscillations. Figure 2 shows part of the time series for the piezometer P10, which will be used as the reference output time series for the rest of study. The chosen piezometer is far enough from the coast (about 500 meters) for not being reached by tidal waves. This is shown in Figure 3 where the spectral density functions of the observed groundwater head and tidal time series are displayed. The tidal spectrum shows two significant peaks accordingly with the periods of 12 and 24 hours of the spring and neaps recorded at the Lagoon. The same shape of the spectral density function is noticeable for the groundwater head time series observed in P1, which is very near to the coast (about 30 meters). On the contrary, the spectrum for the time series in P10 is significantly different, and the major peak at a period of 24 hours accounts for to the daily fluctuations induced by the evapotranspiration phenomenon.

4.2. Groundwater evapotranspiration

In shallow groundwater systems, vegetated soil evapotranspiration extract water from both the unsaturated and the saturated zone (Lautz, 2008). In these circumstances, the water table presents typical diurnal fluctuations, as shown in Figure 4 for the P10 time series. The partitioning between vadose zone evapotranspiration and groundwater evapotranspiration depends on soil and vegetation parameters, but it is also controlled dynamically by depth to water table. In fact, decreases in the hydraulic head cause an exponential decay of groundwater evapotranspiration which reaches a value of zero at a certain depth, namely the extinction depth (Shah et al., 2007). In this study, the FAO56 Penman-Monteith equation was employed to estimate hourly reference evapotranspiration in the study site (Allen et al., 1998). Hourly average observations of temperature, relative humidity, solar radiation and wind speed, have thus been gathered from a meteorological station of ARPAV (Agenzia Regionale Protezione Ambiente del Veneto) in Cavallino-Treporti, placed about 5 km northeast of the site. The Penman-Monteith equation assumes an hypothetical grass surface whereas land cover in Punta Sabbioni also presents a patched mixture of bare soil and vegetables crop. However, this simplifying assumption is acceptable for the chosen piezometer although further considerations would be needed when modelling time series recorded at the other piezometers of the monitoring network.

4.3. Rainfall

Rainfall events cause abrupt shifts in groundwater head for the inward piezometers in Punta Sabbioni. Groundwater recharge due to rainfall is a complex process, as it involves water infiltration through the unsaturated zone (Viswanathan, 1983). Although this process is very slow, for shallow phreatic aquifers infiltration may reach groundwater relatively quickly, and small delays occurs between the individual rainfalls and an increase in the water table elevation (Wu et al., 1996). To model these dynamics, hourly total rainfall data was collected from the meteorological station of ISAC CNR (Institute of Atmospheric Sciences and Climate of the Italian National Research Council) placed close to the construction site of Punta Sabbioni (Magistrato delle Acque di Venezia, 2008). Missing observations were integrated with recordings of two stations of the ARPAV monitoring network: the one in Cavallino-Treporti, and another one at Istituto Cavanis, sited around 8 km west from Punta Sabbioni.

5. Methodology

As stated in the introduction, our aim is to develop a neural network model which is able to reproduce groundwater fluctuations for long periods using the observed time series of the external variables. To perform the system identification, the neural model is first trained to perform 1-hour ahead predictions of the groundwater table depth using past observed groundwater levels as well. Once this autoregressive model has been developed, simulations are produced by feeding back its output as the simulation times increases. Therefore, the better the model will perform on prediction, the better will be its simulation performances.

5.1. Input selection

The predictive ability of ANNs depends heavily on the choice of the input set, which should ideally contain only variables with explanatory potential. In fact, including irrelevant or redundant variables results in larger models which are more difficult to train and less accurate. Furthermore, this issue is particularly critical when employing FNNs for time series applications, since timelagged autoregressive and exogenous inputs must be explicitly provided to explain the behaviour of dynamical systems (Maier and Dandy, 2000). For these reasons, insights on the causal relationship between groundwater fluctuations and the external variables have been obtained by the analysis presented in the previous section, which defined rainfall and evapotranspiration as the external inputs for determining groundwater fluctuations. The experimental data set consisted of a total of 23850 triple hourly observations, ranging from the 11 October 2005 to 30 June 2008. The data set has been split to create a training data set, which is arranged for model calibration, and a validation data set, where the model showing the best performances in the training data set will be used to perform the simulation. In order to estimate the proper autoregressive order and external input delays for the FNN, the training data set is in turn divided in two chunks and the following procedure is exploited. The majority of data patterns are used to estimate several linear Auto-Regressive with eXogenous inputs (ARX) models using a different range of orders and delays. Their performances are then evaluated on the remaining observations, composing what we named the order selection data set, and the best performing model according to the Akaike Information Criterion (AIC) (Akaike, 1974) is selected. The autoregressive order and input delays of the FNN will be those of this best performing ARX model, which will also be used as a benchmark for the application. A similar procedure for selecting the FNN inputs has been reported by Coulibaly et al. (2000), though the authors made use of an Auto-Regressive Moving Average with eXogenous inputs (ARMAX) instead. Several combinatorial trials done on the FNNs to estimate the optimal input set have indicated that there are no major improvements in using orders and lags different than those obtained with the ARX procedure. However, more systematic approaches for input and lag selection have been proposed in the literature (Bowden et al., 2005), and should be employed especially when dealing with higher dimensional input domains. The overall data set subdivision is reported in Table 1.

5.2. Model calibration

Once the inputs and relative lags have been selected, the optimal network architecture is determined by choosing the number of units in the hidden layer. The neural network should be large enough to capture the underlying regularities in the data, but not too large in order to prevent a loss of generalization due to over fitting in the training data set. In this study, the optimal number of hidden nodes is selected by trial and error. Due to the high number of available observations, cross validation on an independent data set has not been exploited to avoid overfitting (Amari et al., 1997). However, performances being similar, the optimal model would be the one with the fewer number of hidden neurons.

5.3. Choice of performance criteria

For a complete assessment of model performances both an absolute and a relative error measure have been used, namely the root mean square error (RMSE)

$$RMSE = \sqrt{\frac{1}{N}\sum_{t=1}^{N}\left(y_t - \hat{y}_t\right)^2}\,, \tag{4}$$

and Nash-Sutcliffe Coefficient of Efficiency (COE) (Legates and McCabe, 1999)

$$COE = 1 - \frac{\sum_{t=1}^{N}\left(y_t - \hat{y}_t\right)^2}{\sum_{t=1}^{N}\left(y_t - \overline{y}\right)^2}\,, \tag{5}$$

where y_t are the observed outputs, $\overline{y}$ is the observed mean, $\hat{y}_t$ are the FNN predicted outputs and N is the number of observations. Accurate models would show values of RMSE close to zero and of COE near to one.

6. Results and discussion

According to the discussion in 5.1, the data were divided into training, order selection and validation sets, as shown in Table 1. Several linear models have then been developed to estimate the optimal autoregressive orders and input lags using the AIC criterion. The model with the highest AIC on the order selection data set was found to be an ARX of order (4, 4, 4), with no time delays for the external inputs. After the regressor array has been defined, neural network models have been developed for the aquifer system identification. Hyperbolic tangents were selected as the activation functions for the hidden layer since they have been found to provide better accuracy with respect to other sigmoids (Kalman and Kwasny, 1992; Maier and Dandy, 1998). The output neuron was chosen as linear because some authors have suggested to employ such activation function in the output layer for forecasting applications (Zhang et al., 1998). The training procedure has been performed with the Levenberg-Marquardt method (Coulibaly et al., 2000). The training was stopped either when a maximum iterations of 200 was reached, or when the prediction error on the calibration data set was below a fixed threshold. To determine the optimal size of the hidden layer, several FNN models with different number of hidden neurons (from 2 to 20) were sequentially trained on the calibration data set. The best model in terms of prediction performances was found to have 4 hidden neurons, and its characteristics are given in Table 2. The neural network simulation performances on both the training and validation data sets are reported in Table 3, along with the results obtained with the ARX model. It should be noted first that both models fits the data equally well when employed for 1-hour ahead predictions, with values of COE equal to 1. However, the performances differ substantially when the models are employed for simulation, with the FNN significantly outperforming the ARX in both terms of RMSE and COE. The RMSE computed for the FNN outputs in the training data set is slightly above 9 cm, which is half of the figure computed for the ARX model. The two values are respectively one-fourth and one-half of the observed standard deviation, which is around 36 cm. In the same way, the COE value for the FNN (0.938) is significantly higher than that of the ARX model (0.764), indicating a stronger correlation between the FNN output and the observed data. Both models suffer a natural loss of performance on the validation data set, however the neural network provides overall better accuracy and efficiency with respect to the linear model. From Table 3, it can be seen that the RMSE for the FNN on the validation data set is slightly above 5 cm, around 43% of the observed standard deviation of 12 cm. This value is again around one-half of the computed RMSE for the ARX model, which is above 9 cm and amounts to 77% of the observed standard deviation. Accordingly, the COE of the ARX model on the validation data drops to 0.527, while the efficiency of the neural network is still a satisfactory 0.809. The difference in the performances of the two models can also be appraised by a visual inspection of the simulated and real outputs, as shown in Fig.5 and Fig.6 for the validation data set. It can be seen that the output of the neural model is overall closer to the observations. In particular, the FNN tends to slightly overestimate some rainfall events, while the ARX model underestimate groundwater levels for much longer periods. It is worth noting that for the period going from 8 May 08 to 15 June 08, reported in Fig. 6, rainfall data on the study site was missing, and it was integrated with the recordings of another meteorological station. As a matter of fact, when employing such data as input, the precision of the results varies depending on the difference in timing, duration and intensity of the meteoric events occurring at the different locations, determined by the distance between them (around 8 km). As regards the effects of evapotranspiration on groundwater dynamics, it can be seen from the enlargement in Fig. 7 that both models account for the downward trends and daily oscillations in groundwater levels, suggesting that the reference evapotranspiration obtained with the Penman-Monteith equation is a consistent input for modelling groundwater evapotranspiration in shallow unconfined aquifers.

7. Conclusions

In this work, feed forward neural networks (FNNs) have been employed to perform long simulations of hourly groundwater levels recorded at coastal unconfined aquifer in the Lagoon of Venice, Italy. The developed FNN has been first trained to perform one-step ahead predictions using past observed groundwater data along with the external inputs. After the training, simulations were produced by feeding back the outputs computed by the FNNs run-time in place of past observed data. In this way, the study has assessed the ability of FNNs to produce accurate groundwater level simulations for long periods, at least six months, relying only on the external data gathered on site. Furthermore, the developed FNN clearly outperform the linear ARX model which has been employed for comparison. The consistency of the output produced by the FNNs justifies practical applications such as testing of the future aquifer responses under plausible scenarios or the reconstruction of long periods of missing groundwater level observations, provided external data such as rainfall and evapotranspiration is available. In a future paper, we aim to compare the results obtained with the FNN with a numerical model of the aquifer system which is currently under development.

Acknowledgements

The monitoring activities were financed by Magistrato delle Acque di Venezia, and coordinated by CORILA. We want to acknowledge Pierpaolo Campostrini and Caterina Dabalà of CORILA, Franco Belosi of ISAC CNR and Alessandro Casasso, Tommaso Baldarelli, Chiara Santi, Silvia Delforno for the maintenance of the data set over time.

Bibliography

Akaike, H., 1974. A new look at the statistical model identification. IEEE Transactions on Automatic Control, 19(6): 716-723.

Allen, R.G., Pereira, L.S., Raes, D. and Smith, M., 1998. Crop evapotranspiration: guidelines for computing crop water requirements. United Nations Food and Agriculture Organization, Irrigation and Drainage Paper 56, Rome, Italy.

Amari, S.-i., Murata, N., Müller, K.-R., Finke, M. and Yang, H.H., 1997.Asymptotic statistical theory of overtraining and cross-validation. IEEE Transactions on Neural Networks 8(5): 985-996.

ASCE Task Committee on Application of Artificial Neural Networks in Hydrology, 2000. Artificial neural networks in hydrology, parts I and II. Journal of Hydrologic Engineering, 5(2): 115-137.

Bowden, G.J., Dandy, G.C. and Maier, H.R., 2005. Input determination for neural network models in water resources applications. Part 1 - background and methodology. Journal of Hydrology, 301(1-4): 75-92.

Bras, R.L., Harleman, D.R.F., Rinaldo, A. and Rizzoli, P., 2001. Rescuing Venice from a watery grave. Science, 291(5512): 2315-2315.

Chau, K.W., Wu, C.L. and Li, Y.S., 2005. Comparison of several flood forecasting models in Yangtze river. Journal of Hydrologic Engineering, 10(6): 485-491.

Cheng, C.T., Chau, K.W., Sun, Y.G. and Lin, J.Y., 2005. Long-term prediction of discharges in Manwan reservoir using artificial neural network models. Lecture Notes in Computer Science, 3498: 1040-1045.

Coulibaly, P., Anctil, F. and Bobee, B., 2000. Daily reservoir inflow forecasting using artificial neural networks with stopped training approach. Journal of Hydrology, 230(3-4): 244-257.

Coulibaly, P., Anctil, F., Aravena, R. and Bobee, B., 2001. Artificial neural network modeling of water table depth fluctuations. Water Resources Research, 37(4): 885-896.

Daliakopoulos, I.N., Coulibaly, P. and Tsanis, I.K., 2005. Groundwater level forecasting using artificial neural networks. Journal of Hydrology, 309(1-4): 229-240.

Dawson, C.W. and Wilby, R., 1998. An artificial neural network approach to rainfall-runoff modelling. Hydrological Sciences Journal-Journal Des Sciences Hydrologiques, 43(1): 47-66.

Haykin, S., 1998. Neural networks: a comprehensive foundation (2nd Edition) Prentice Hall.

Hornik, K., Stinchcombe, M. and White, H., 1989. Multilayer feedforward networks are universal approximators. Neural Networks, 2(5): 359-366.

Hsu, K.L., Gupta, H.V. and Sorooshian, S., 1995. Artificial neural-network modeling of the rainfall-runoff process. Water Resources Research, 31(10): 2517-2530.

Joorabchi, A., Zhang, H. and Blumenstein, M., 2007. Application of artificial neural networks in flow discharge prediction for the Fitzroy River, Australia. Journal of Coastal Research, SI, 50: 287-291.

Kalman, B.L. and Kwasny, S.C., 1992. Why Tanh? Choosing a sigmoidal function. In: Proceedings of the International Joint Conference on Neural Networks, Baltimore, MD IEEE, New York, Vol. 4:578-581.

Lautz, L.K., 2008. Estimating groundwater evapotranspiration rates using diurnal water-table fluctuations in a semi-arid riparian zone. Hydrogeology Journal, 16(6): 483-497.

Legates, D.R. and McCabe, G.J., 1999. Evaluating the use of "goodness-of-fit" measures in hydrologic and hydroclimatic model validation. Water Resources Research, 35(1): 233-241.

Magistrato delle Acque di Venezia, 2008. Studio B.6.72 B/4. Attività di rilevamento per il monitoraggio degli effetti prodotti dalla costruzione delle opere alle bocche lagunari. Consorzio Venezia Nuova - Esecutore CORILA.

Maier, H.R. and Dandy, G.C., 1997. Determining inputs for neural network models of multivariate time series. Computer-Aided Civil and Infrastructure Engineering, 12(5): 353-368.

Maier, H.R. and Dandy, G.C., 1998. The effect of internal parameters and geometry on the performance of back-propagation neural networks: An empirical study. Environmental Modelling & Software, 13(2): 193-209.

Maier, H.R. and Dandy, G.C., 2000. Neural networks for the prediction and forecasting of water resources variables: a review of modelling issues and applications. Environmental Modelling & Software, 15(1): 101-124.

Maier, H.R., Jain, A., Dandy, G.C. and Sudheer, K.P., 2010. Methods used for the development of neural networks for the prediction of water resource variables in river systems: Current status and future directions. Environmental Modelling & Software, 25(8): 891-909.

May, D.B. and Sivakumar, M., 2009. Prediction of urban stormwater quality using artificial neural networks. Environmental Modelling & Software, 24(2): 296-302.

Muttil, N. and Chau, K.W., 2006. Neural network and genetic programming for modelling coastal algal blooms. International Journal of Environment and Pollution, 28(3-4): 223-238.

Nayak, P.C., Rao, Y.R.S. and Sudheer, K.P., 2006. Groundwater level forecasting in a shallow aquifer using artificial neural network approach. Water Resources Management, 20(1): 77-90.

Nourani V., Mogaddam A.A. and Nadiri A.O., 2008. An ANN-based model for spatiotemporal groundwater level forecasting. Hydrological Processes, 22(26): 5054-5066.

Nourani V, Ejlali R.G. and Alami M.T., 2011. Spatiotemporal groundwater level forecasting in coastal aquifers by hybrid artificial neural network-geostatistics model: a case study. Environmental Engineering Science, 28(3): 217-228.

Rinaldo, A., Nicotina, L., Alessi Celegon, E., Beraldin, F., Botter, G., Carniello, L., Cecconi, G., Defina, A., Settin, T., Uccelli, A., D'Alpaos, L., Marani, M., 2008. Sea level rise, hydrologic runoff, and the flooding of Venice. Water Resources Research, 44(2): Article number W12434.

Shah, N., Nachabe, M. and Ross, M., 2007. Extinction depth and evapotranspiration from ground water under selected land covers. Ground Water, 45(3): 329-338.

Trichakis I.C., Nikolos I.K. and Karatzas G.P., 2009. Optimal selection of artificial neural network parameters for the prediction of a karstic aquifer’s response. Hydrological Processes, 23(20): 2956–2969.

Viswanathan, M.N., 1983. The rainfall water-table level relationship of an unconfined aquifer. Ground Water, 21(1): 49-56.

Wu, J.Q., Zhang, R.D. and Yang, J.Z., 1996. Analysis of rainfall-recharge relationships. Journal of Hydrology, 177(1-2): 143-160.

Zhang, B.E., Patuwo, B.E. and Hu, M.Y., 1998. Forecasting with artificial neural networks: the state of the art. International Journal of Forecasting, 14(1): 35–62.

Figure captions

Fig. 1. The Venetian Lagoon and the case study area with the Mo.S.E. construction site.

Fig. 2. Hourly groundwater levels recorded in the piezometers P10.

Fig. 3. Spectral density of groundwater level and tidal data.

Fig. 4. Daily fluctuations in P10 due to groundwater evapotranspiration.

Fig. 5. Comparison of observed and simulated data on the first half of the validation data set.

Fig. 6. Comparison of observed and simulated data on the second half of the validation data set .

Fig. 7. Simulation of groundwater head fluctuations in P10 due to evapotranspiration.

Tables

data set	from	to	# observations
training	11/10/2005	10/10/2007	17500
order selection	11/10/2007	10/01/2008	2200
validation	11/01/2008	30/06/2008	4150

Table 1. Experimental data subdivision in training, order selection and validation data set.

FNN	
# parameters	57
# hidden units	4
# inputs	12
Type of input	lag (hours)
Rainfall	0, 1, 2, 3
Evapotranspiration	0, 1, 2, 3
Water level	1, 2, 3, 4

Table 2. Description of the neural network model and selected inputs.

Model	COE		RMSE (cm)		RMSE/σ	
	Training	Validation	Training	Validation	Training	Validation
ARX444	0.764	0.527	18.1	9.3	0.503	0.775
FNN	0.938	0.809	9.2	5.2	0.256	0.433

Table 3. Simulation performances of the FNN and ARX models on the training and validation data set.

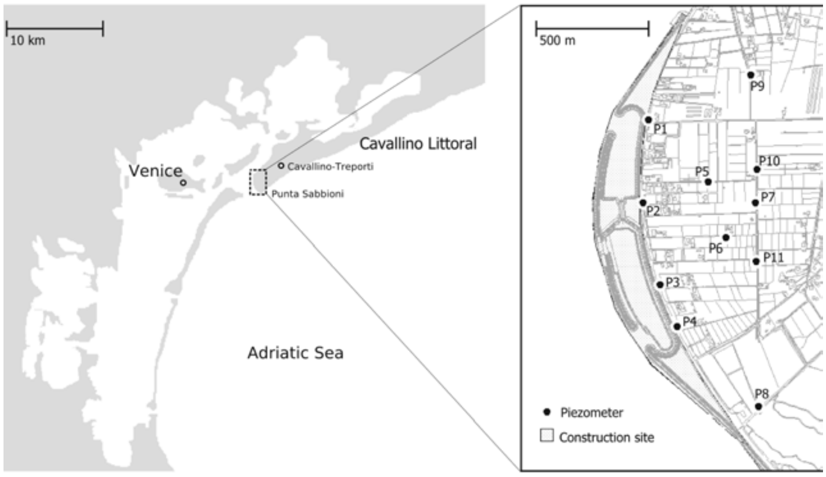
10 km
Venice
Cavallino Littoral
Cavallino-Treporti
Punta Sabbioni
Adriatic Sea
500 m
P9
P1
P10
P5
P7
P2
P6
P11
P3
P4
P8
Piezometer
Construction site

Figure 1.

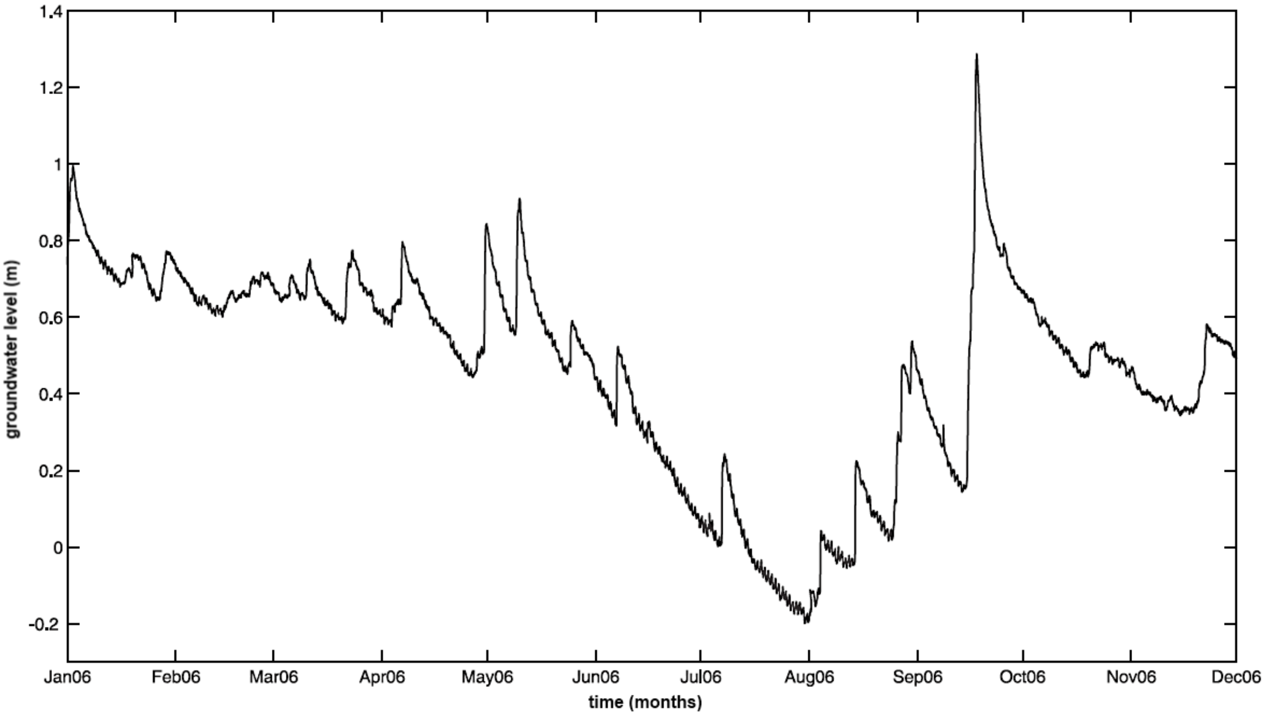
groundwater level (m)
time (months)
1.4
1.2
1
0.8
0.6
0.4
0.2
0
-0.2
Jan06
Feb06
Mar06
Apr06
May06
Jun06
Jul06
Aug06
Sep06
Oct06
Nov06
Dec06

Figure 2.

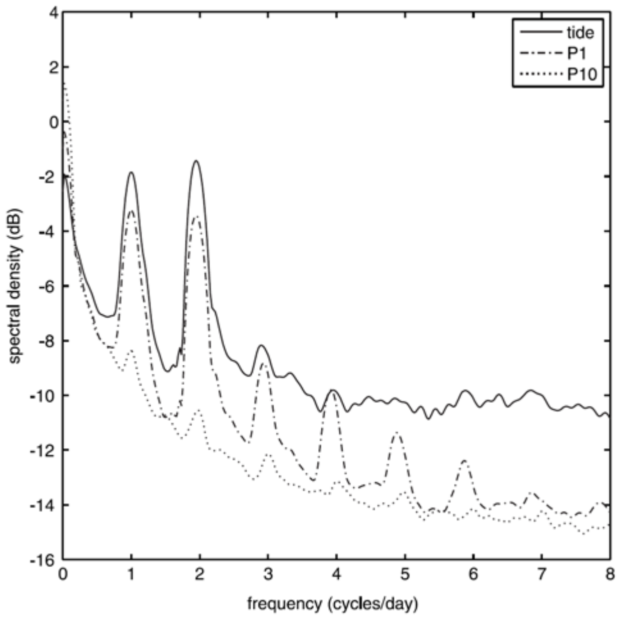
tide
P1
P10
spectral density (dB)
frequency (cycles/day)
4
2
0
-2
-4
-6
-8
-10
-12
-14
-16
0
1
2
3
4
5
6
7
8

Figure 3.

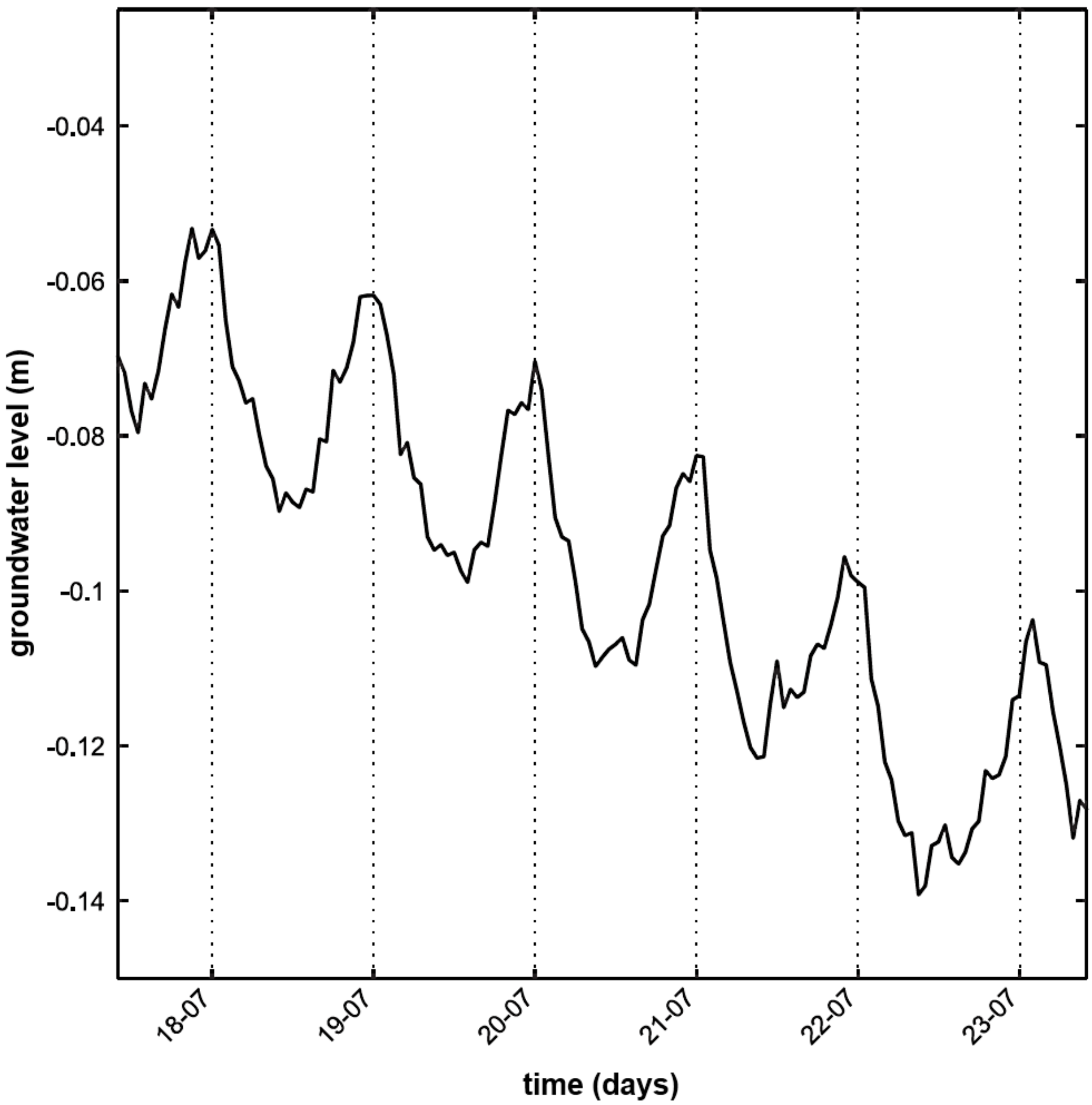
-0.04
-0.06
-0.08
-0.1
-0.12
-0.14
groundwater level (m)
18-07
19-07
20-07
21-07
22-07
23-07
time (days)

Figure 4.

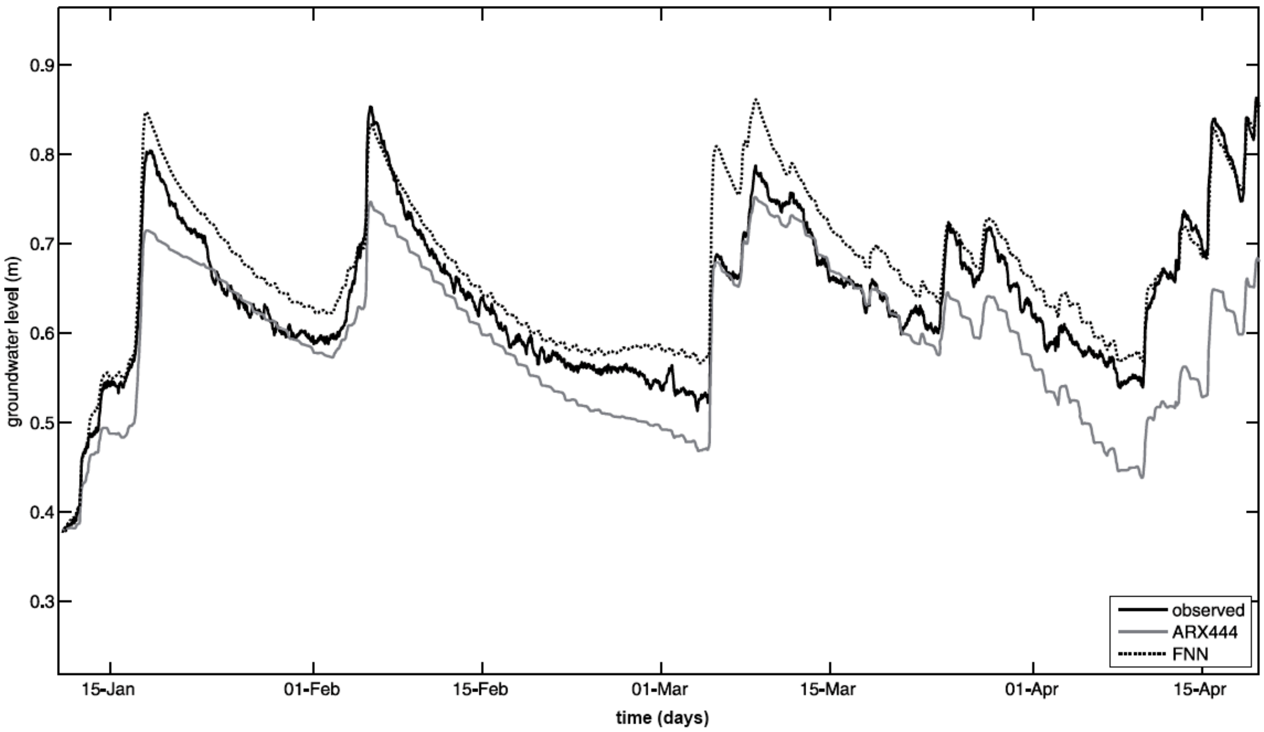
0.9
0.8
0.7
0.6
0.5
0.4
0.3
groundwater level (m)
15-Jan
01-Feb
15-Feb
01-Mar
15-Mar
01-Apr
15-Apr
time (days)
observed
ARX444
FNN

Figure 5.

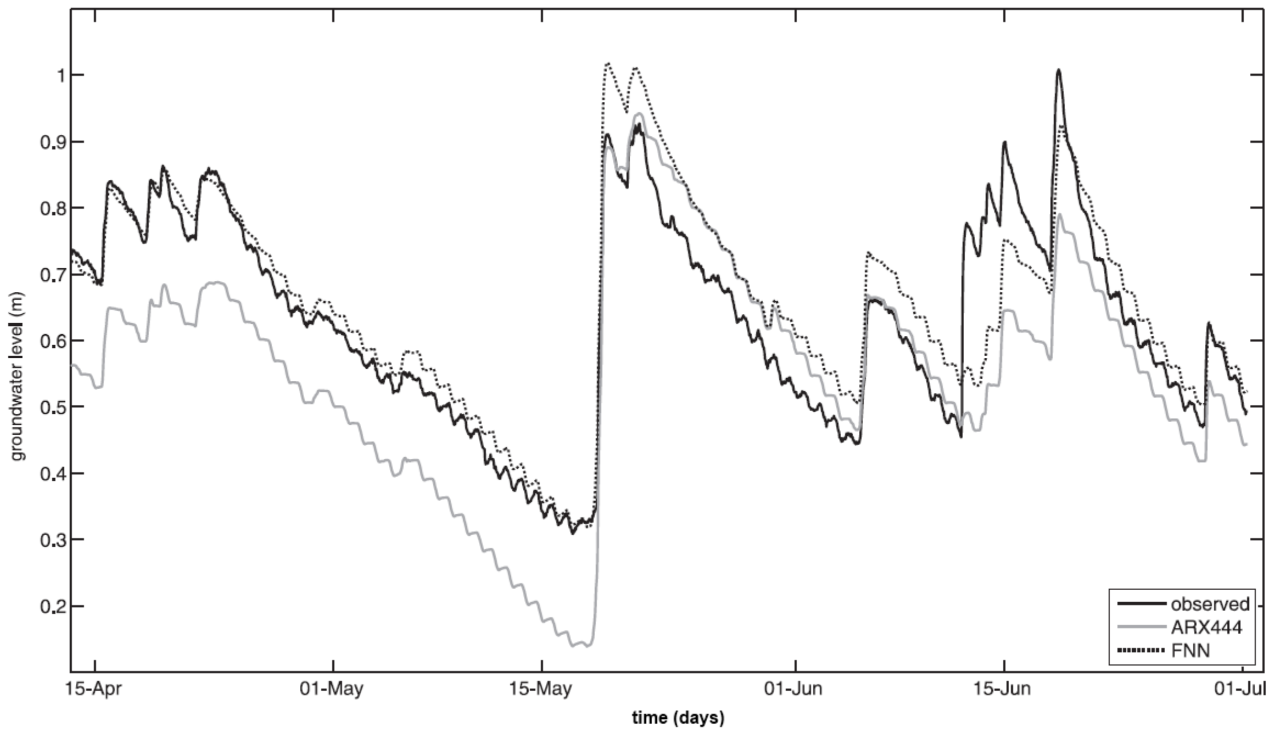
groundwater level (m)
1
0.9
0.8
0.7
0.6
0.5
0.4
0.3
0.2
15-Apr
01-May
15-May
01-Jun
15-Jun
01-Jul
time (days)
observed
ARX444
FNN

Figure 6.

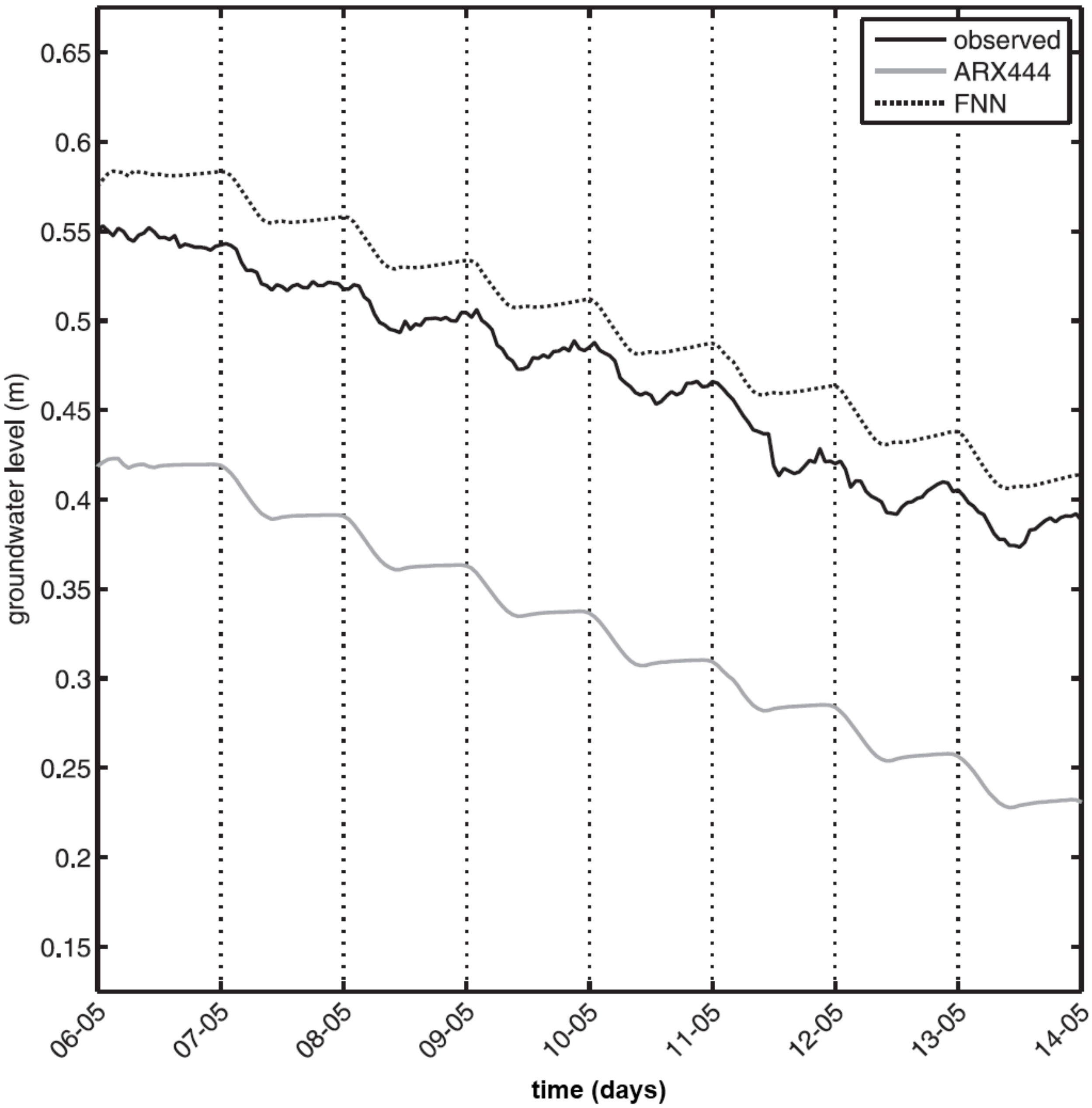
observed
ARX444
FNN
0.65
0.6
0.55
0.5
0.45
0.4
0.35
0.3
0.25
0.2
0.15
groundwater level (m)
06-05
07-05
08-05
09-05
10-05
11-05
12-05
13-05
14-05
time (days)

Figure 7.